

## SECIS element variability and its role in selenocysteine versus cysteine utilization in SelD enzymes

Masao Inoue, Riku Aono, Anna Ochi, Yukiko Izu, Toma Rani Majumder, Ming Li, Hisaaki Mihara\*

Department of Biotechnology, College of Life Sciences, Ritsumeikan University

### Abstract

Selenophosphate synthetase SelD from *Haemophilus influenzae* (HinSelD) has a selenocysteine (Sec) residue at its active site, while its *Escherichia coli* homolog (EcoSelD), which shares 65% amino acid sequence identity, contains cysteine (Cys) instead. This difference prompts questions about the evolutionary divergence between Sec-type and Cys-type SelD enzymes. We used bioinformatics tools to compare the selenocysteine insertion sequence (SECIS) elements of the Sec-type *selD* gene with the corresponding sequence regions of the Cys-type genes. Our analysis showed vital conservation between the UGA Sec codon and SECIS secondary structures. We also tested if HinSelD SECIS could support Sec insertion in *E. coli*. Results indicated that HinSelD SECIS is recognized by *E. coli*, enabling Sec incorporation. Nucleotide differences between HinSelD and EcoSelD SECIS regions affected translation efficiency, with mutants G69A, A75G, G77A, and U84C showing 93%, 81%, 69%, and 69% of wild-type translation levels, respectively. Additionally, the Sec16Cys mutant of HinSelD exhibited a similar expression level compared to the wild-type, suggesting the secondary structure of the SECIS does not inhibit the translation of the preceding UGC codon for Cys.

**Keywords:** selenocysteine, SECIS element, selenophosphate synthetase, cysteine, bacteria

**Statements about COI:** The authors have no conflicts of interest associated with this manuscript to declare.

### \*Correspondence

Hisaaki Mihara  
Department of Biotechnology, College of Life Sciences,  
Ritsumeikan University, 1-1-1 Nojihigashi, Kusatsu,  
Shiga 525-8577, Japan

Tel ; +81 77 561 2732

E-mail ; [mihara@fc.ritsumeik.ac.jp](mailto:mihara@fc.ritsumeik.ac.jp)

Received: October 22, 2024

Accepted: December 23, 2024

Released online: January 08, 2025

### Introduction

Selenium is an essential trace element incorporated into proteins as the selenocysteine (Sec) residue, which plays a crucial role in biological functions [1]. Proteins that specifically incorporate Sec are known as selenoproteins, characterized by their high catalytic activity, making them promising for industrial and pharmaceutical applications. In bacteria, the insertion of Sec into proteins involves four genes: *selA*, *selB*, *selC*, and *selD* [2]. The *selC* gene encodes a tRNA specific for Sec, known as tRNA<sup>Sec</sup>, which is charged by seryl-tRNA synthetase (SerRS) to form seryl-tRNA<sup>Sec</sup> [3]. The selenophosphate synthetase SelD catalyzes the formation of selenophosphate from selenide and ATP



This work is licensed under a Creative Commons Attribution 4.0 International License.

©2025 THE AUTHORS. [DOI](https://doi.org/10.11299/metallomicsresearch.MR202408) <https://doi.org/10.11299/metallomicsresearch.MR202408>

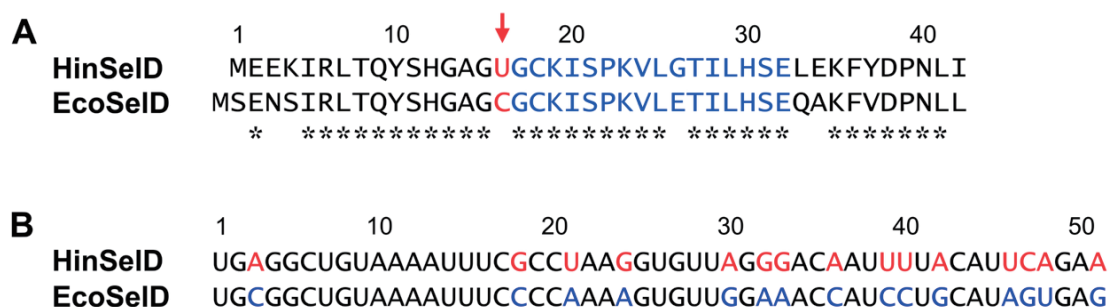


**Figure 1. Comparison of the N-terminal amino acid sequences and SECIS element nucleotide sequences of EcoSelD and HinSelD**

(A) Arrows and red text indicate the positions of Sec16 (U) in HinSelD and Cys17 (C) in EcoSelD. Conserved amino acid residues are marked with an asterisk (\*), and the amino acid sequences encoded by the SECIS region are highlighted in blue. (B) Nucleotide sequences of the SECIS element in the HinSelD gene and the corresponding region in the EcoSelD gene. Nucleotide differences in the SECIS element of HinSelD and corresponding region of EcoSelD are highlighted in red and blue, respectively.

[4]. The enzyme Sec synthase SelA then converts seryl-tRNA<sup>Sec</sup> and selenophosphate into Sec-tRNA<sup>Sec</sup> [2]. On the mRNA of selenoproteins, an in-frame UGA codon is present, along with a selenocysteine insertion sequence (SECIS) element that adopts a stem-loop secondary structure, essential for translating UGA as a Sec codon rather than a stop codon [5]. The specialized translation elongation factor SelB interacts with SECIS, Sec-tRNA<sup>Sec</sup>, and the ribosome, facilitating the insertion of Sec at the UGA codon [5]. Bacterial SECIS elements share several conserved features: the apical loop, located 16–37 nucleotides downstream of the UGA codon, comprises 3–14 nucleotides and contains at least one guanine (G) residue [6]. Below the apical loop is a stem structure of 4–16 base pairs.

Selenophosphate synthetase SelD with a Sec residue at the active site has been identified in *Haemophilus influenzae* (HinSelD) [7]. HinSelD shares a high sequence homology with *Escherichia coli* SelD (EcoSelD), with 65% identity at the amino acid level. The Sec16 residue in HinSelD corresponds to a cysteine residue (Cys17) in EcoSelD [8]. The surrounding amino acid sequences around the Sec in HinSelD and the Cys in EcoSelD are highly conserved (Figure 1A). A comparison of the nucleotide sequences of the SECIS elements between EcoSelD and HinSelD revealed a few nucleotide substitutions, but overall conservation was observed (Figure 1B). This observation raises intriguing questions regarding the evolutionary divergence between Sec-type and Cys-type SelD enzymes. In this study, bioinformatics approaches were used to compare the nucleotide sequences and secondary structures of the SECIS regions in Sec-type and Cys-type SelDs from different microorganisms, revealing a high degree of conservation between the presence of the UGA Sec codon and the characteristic secondary structures of the SECIS elements. In addition, we introduced nucleotide substitution in the SECIS element of the HinSelD gene to produce variants, G69A, A75G, G77A, and U84C, based on the comparison with the same region of the EcoSelD gene. The G69A, A75G, G77A, and U84C mutants exhibited translation product levels of 93%, 81%, 69%, and 69%, respectively, of the wild-type, suggesting some flexibility in the recognition of HinSelD SECIS by the *E. coli* translation system. Furthermore, in the Sec16Cys mutant of HinSelD, there was no significant change in expression levels compared to the wild-type, suggesting the secondary structure of the SECIS does not inhibit the translation of the preceding UGC codon for Cys.

## Materials and methods

### Phylogenetic analysis

The amino acid sequence of HinSelD (R2866\_0388) was used as a query for a BLASTp [9] search in KEGG (<https://www.genome.jp/kegg/>) to retrieve sequences from SelD proteins of 19 *Pasteurellales* species and 14 *Enterobacterales* species, including various *Haemophilus* and *Mannheimia* species. Sequences with shifted start codons, such as

*Haemophilus pittmaniae* (NCTC13334\_01230), *Haemophilus parainfluenzae* (PARA\_00030), and *Mannheimia succiniciproducens* (MS1241), were manually corrected to obtain full-length sequences. An outgroup, *Geobacter sulfurreducens* Seld (gsu0607), was included in the alignment. Multiple sequence alignment was performed using Muscle on MEGA7 [10], and a maximum-likelihood phylogenetic tree was constructed using IQ-TREE2 with the LG+G4 model [11]. Bootstrap values were calculated with 1,000 replications using SH-aLRT [12] and Ultrafast Bootstrap [13]. The phylogenetic tree was visualized using iTOL v6 [14].

### RNA secondary structure prediction

In the HinSeld gene (R2866\_0388), the SECIS element was defined as the 51 nt sequence starting from the 5' end of the UGA codon for selenocysteine (**Figure 1A**). SECIS-like sequences were extracted from the 34 *seld* gene sequences based on multiple sequence alignment. RNA secondary structures of these SECIS-like sequences were predicted using the MXfold2 Server (<http://www.dna.bio.keio.ac.jp/mxfold2/>) [15].

### Bacterial strain, culture conditions, and preparation of crude extracts

*E. coli* BL21(DE3) cells transformed with an expression plasmid were cultured in Luria-Bertani (LB) medium containing 0.3% glucose, 1  $\mu$ M sodium selenite, 10  $\mu$ M sodium molybdate hydrate, and 100  $\mu$ g/mL ampicillin at 37°C with shaking until the OD<sub>600</sub> reached 0.55–0.64. Protein expression was induced by adding 0.1 mM isopropyl  $\beta$ -D-thiogalactopyranoside (IPTG) or 0.4% lactose, followed by incubation at either 37°C or 30°C for 6 h, with shaking or static conditions. After incubation, cells were harvested by centrifugation, washed twice with phosphate-buffered saline (PBS), and disrupted using ultrasonic sonication UP50H (Hielscher, Teltow, Germany). The lysate was centrifuged at 15,000  $\times g$  for 10 min at 4°C. The supernatant was collected as a crude extract.

### Plasmid construction

The expression plasmid for HinSeld, pET21aHinSeld, was obtained through synthetic gene production by GenScript (Piscataway, NJ, USA). The expression plasmid for EcoSeld, pET21aEcoSeld, was constructed by inserting the *E. coli seld* gene fragment into the NdeI and BamHI sites of pET21a(+) (Merck KGaA, Darmstadt, Germany). Site-specific mutations in the HinSeld expression plasmid pET21aHinSeld were introduced by GenScript.

### Western blotting

Proteins separated by sodium dodecyl sulfate polyacrylamide gel electrophoresis (SDS-PAGE) were transferred to polyvinylidene difluoride (PVDF) membranes (Immobilon-P, Merck Millipore, MA, USA) using a TransBlot SD Semi-dry Transfer Cell (Bio-Rad, CA, USA). An anti-His tag antibody (monoclonal antibody 9C11, FUJIFILM Wako Pure Chemical Corporation, Osaka, Japan) was used as a primary antibody at 1,000-fold dilution. For secondary antibody, anti-mouse IgG(H+L) (Peroxidase Labeled Goat anti-Mouse IgG(H+L) Human Serum Adsorbed, KPL Antibodies & Conjugates, SeraCare, MA, USA) was used at a 14,000-fold dilution. Detection was performed using chemiluminescence (Chemi-Lumi One Super, Nacalai Tesque, Kyoto, Japan) and analyzed with an imaging system (Amersham Imager 600, Cytiva, MA, USA). The band intensities were quantified using ImageJ software [16].

## Results and discussion

### Phylogenetic analysis of Seld

To investigate the evolutionary relationships between Sec-containing and Cys-containing Seld enzymes, a molecular phylogenetic tree was constructed for Seld enzymes from 34 bacterial species, including those from the order Pasteurellales (which includes *H. influenzae*) and the order Enterobacterales (which includes *E. coli*) (**Figure 2**). The analysis revealed that *Pasteurellales* species harbor both Sec-type and Cys-type Seld enzymes, indicating a diverse evolutionary adaptation within this order. In contrast, Seld enzymes in *Enterobacterales* are predominantly Cys-type, suggesting a possible loss or replacement of the Sec residue during evolution in this lineage.

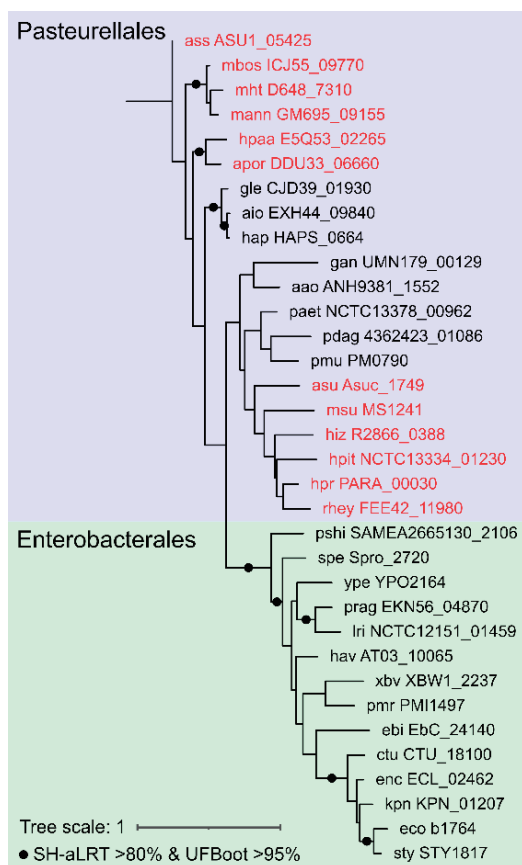


**Figure 2. Phylogenetic tree of SelD from 34 bacterial species**

Selenocysteine-containing SelD enzymes are indicated in red, while cysteine-containing SelD enzymes are shown in black. SelD sequences used were from *Haemophilus pittmaniae* (NCTC13334\_01230), *Haemophilus parainfluenzae* (PARA\_00030), *Rodentibacter heyltii* (FEE42\_11980), *Mannheimia succiniciproducens* (MS1241), *Actinobacillus succinogenes* (Asuc\_1749), *Pasteurella aerogenes* (NCTC13378\_00962), *Pasteurella multocida* (PM0790), *Pasteurella dagmatis* (4362423\_01086), *Aggregatibacter actinomycetemcomitans* (ANH9381\_1552), *Gallibacterium anatis* (UMN179\_00129), *Glaesserella parasuis* (HAPS\_0664), *Actinobacillus indolicus* (EXH44\_09840), *Glaesserella* sp. 15-184 (CJD39\_01930), *Actinobacillus porcitosillarum* (DDU33\_06660), *Haemophilus paraahaemolyticus* (E5Q53\_02265), *Actinobacillus suis* (ASU1\_05425), *Mannheimia bovis* (ICJ55\_09770), *Mannheimia ovis* (GM695\_09155), *Mannheimia haemolytica* (D648\_7310), *Escherichia coli* (b1764), *Salmonella enterica* (STY1817), *Klebsiella pneumoniae* (KPN\_01207), *Enterobacter cloacae* (ECL\_02462), *Cronobacter turicensis* (CTU\_18100), *Erwinia billingiae* (EbC\_24140), *Proteus mirabilis* (PMI1497), *Xenorhabdus bovienii* (XBW1\_2237), *Hafnia alvei* (AT03\_10065), *Leminorella richardii* (NCTC12151\_01459), *Jinshanibacter zhutongyui* (EKN56\_04870), *Yersinia pestis* (YPO2164), *Serratia proteamaculans* (Spro\_2720), and *Plesiomonas shigelloides* (SAMEA2665130\_2106).

### Secondary structure prediction of SECIS elements in SelD genes

We predicted the secondary structures of the SECIS elements and corresponding regions (in the case of Cys-type SelD) in the *selD* genes from 34 bacterial species. For HinSelD (R2866\_0388), the SECIS was defined as the 51-nt sequence downstream of the UGA codon that encodes the selenocysteine residue (**Figure 1B**). Using multiple sequence alignment, SECIS regions were extracted from the *selD* nucleotide sequences of the 34 species (**Table 1**). The RNA secondary structures of these SECIS regions were predicted using the MXfold2 Server [15] (**Figure 3 & Supplementary Figure S1**). In Sec-type SelDs, such as those from *Actinobacillus suis* and HinSelD, the predicted secondary structures conformed to the consensus model for SECIS elements. Conversely, in Cys-type SelDs, including EcoSelD, the predicted secondary structures differed significantly from those of the Sec-type SECIS (**Figure 3**). For instance, in the Cys-type *Glaesserella* sp. SelD, the predicted structure resembled the SECIS secondary structure but lacked the characteristic apical loop guanine (G) and had only three base pairs in the stem, deviating from the typical SECIS model. These findings suggest a high degree of conservation between the presence of the UGA codon for Sec and the characteristic secondary structure of SECIS. A comparative analysis of nucleotide sequences specifically focused on the SECIS regions of Sec-type SelD enzymes is shown in **Figure 4A**. The secondary structure predicted from this consensus sequence is depicted in **Figure 4B** and aligns well with previously proposed bacterial SECIS models [6].

### Investigation of HinSelD SECIS functionality in *E. coli* and optimization of expression conditions

To examine if the HinSelD SECIS is able to be translated in an *E. coli* host translation system, the expression vector pET21aHinSelD, which produces HinSelD with a C-terminal His-tag, and pET21aEcoSelD expressing C-terminal His-tagged EcoSelD were introduced into *E. coli* BL21(DE3) cells, and various expression conditions were tested. The results from SDS-PAGE and western blot analyses of the crude extracts after cultivation showed that increased

**Table 1. | SECIS regions from the *selD* nucleotide sequences of the 34 species**

<i>selD</i> gene ID	SECIS region
ass:ASU1_05425	UGAGGCUGUAAAAUUUCUCCUAAGGUGUUAGGGACAAUUUUACAAAGUCAG
mbos:ICJ55_09770	UGAGGUUGUAAAGAUUUCUCCUAAGGUGUUAGGGACAAUUUUACAAACGCAA
mht:D648_7310	UGAGGCUGUAAAAUUUCGCCUAAGGUGUUAGGGACAAUUUUACAAACUCAA
mann:GM695_09155	UGAGGCUGUAAAAUUUCUCCUAAGGUGUUAGGGACGAUUUUACAAACGCAA
hpa:E5Q53_02265	UGAGGCUGUAAAAUUUCGCCUAAGGUGUUAGGGACAAUUUUACAUAGCGAA
apor:DDU33_06660	UGAGGCUGUAAAAUUUCUCCUAAGGUGUUAGGGACCAUUUUACAAAGCCAA
gle:CJD39_01930	UGC GGUUGUAAAAUUUCCCCAAAAGUGCUUGAGCAAAUUCUGCAUACAGAA
aio:EXH44_09840	UGUGGCUGUAAAAUUUCCCCGAAAGUGCUUGAACAAAUCUACACAUAGAA
hap:HAPS_0664	UGUGGCUGUAAAAUUUCCCCGAAAGUCCUUGAACAAAUCUGCACACAGAA
gan:UMN179_00129	UGC GGUUGUAAAAUUUCCCCAAAAGUUUUAGAAACCAUUCUUCACACAGAA
aao:ANH9381_1552	UGUGGUUGUAAAAUCUCGCCUAAGGUUUAGAGAGUAUUCUGCAUUCAAAA
paet:NCTC13378_00962	UGUGGUUGUAAAAUUUCGCCUAAGUAUUAGAGACGAUUUUGCAUUCCAAC
pdag:4362423_01086	UGUGGGUGUAAAAUUUCACCAAAGUGCUUGAGCAAAUUUUACAUUCUGAA
pmu:PM0790	UGC GGUCUGUAAAAUUUCGCCGAAAGUCCUCGAAAAGAUUUUACACUCUGAC
asu:Asuc_1749	UGAGGCUGUAAAAUUUCGCCUAAGGUUUAGGGACUAAUUUUACAAACGAAA
msu:MS1241	UGAGGCUGUAAAGAUUUCUCCUAAGGUGUUAGGGACUAAUUUUACACAGUCAG
hiz:R2866_0388	UGAGGCUGUAAAAUUUCGCCUAAGGUGUUAGGGACAAUUUUACAUUCAGAA
hpit:NCTC13334_01230	UGAGGCUGUAAAAUUUCGCCUAAGGUGUUAGGGACAAUUUUACAAAGCGAA
hpr:PARA_00030	UGAGGUUGUAAAAUUUCGCCUAAGGUGUUAGGGACAAUUUUACAGACUAAA
rhey:FEE42_11980	UGAGGCUGUAAAAUUUCGCCUAAGGUGUUAGGGACAAUUUUACAAACGCAA
pshi:SAMEA2665130_2106	UGUGGGUGUAAAAUCUCGCCUAAGUGCUGGAUACCAUUCUGCACUCGGAA
spe:Spro_2720	UGC GGUUGUAAAAUCUCACCGAAAGUUCUGGAAACUAAUUCUGCACAGCGAG
ype:YPO2164	UGUGGUUGCAAGAUUUCACCAAAGUUUUGGAUAAAAUUUUGCAUACUGAG
prag:EKN56_04870	UGUGGCUGCAAAAUCUCCCCAAAAGUACUGGAAACGAUCCUGCAUUCUGAG
lri:NCTC12151_01459	UGC GGGUGUAAAAUCUCGCCGAAAGUGUUUGGAAACGAUUCUCCACUCCGAG
hav:AT03_10065	UGUGGAUGUAAAGAUUCUCCCCUAAAGUGUUAGAAACCAUUCUGCACAGCGAA
xbv:XBW1_2237	UGUGGCUGUAAAAUUUCGCCAAAAGUGUUGGAAACUAAUUCUGCACAGUGAG
pmr:PMI1497	UGUGGCUGCAAAAUUUCACCAAAGUUUUGGAAACGAUUUUACAUAGUGAA
ebi:EbC_24140	UGC GGUCUGUAAAGAUUUCACCCAGCGUGCUGGAGACCAUACUGCACAGCGAU
ctu:CTU_18100	UGC GGUUGUAAAAUUUCCCCGAAAGUGCUGGAAACCAUCCUGCACAGCGAU
enc:ECL_02462	UGC GGUUGUAAAAUUUCCCCAAAAGUGCUGGAAACCAUCCUGCACAGUGAA
kpn:KPN_01207	UGUGGUUGUAAAAUUUCCCCGAAAGUGCUGGAAACUAAUCCUGCAUAGCGAG
eco:b1764	UGC GGUCUGUAAAAUUUCCCCAAAAGUGUUGGAAACCAUCCUGCAUAGUGAG
sty:STY1817	UGC GGUUGUAAAAUUUCCCCUAAAGUGCUGGAGACUAAUCCUGCAUAGCGAG



Coomassie Brilliant Blue (CBB)-stained protein bands and immuno-reactive bands around 37 kDa were observed for both HinSelD (calculated molecular mass of 37.2 kDa) and EcoSelD (calculated molecular mass of 37.5 kDa) under IPTG induction, indicating successful expression of HinSelD in *E. coli* (**Figure 5**). This suggests that the HinSelD SECIS is functional for Sec insertion in the *E. coli* host translation system. IPTG induction resulted in higher protein expression levels compared to lactose induction. Based on the results, the optimal expression conditions were determined to be shaking incubation at 37°C with 0.1 mM IPTG, which were employed for subsequent analyses. EcoSelD migrated faster than HinSelD on SDS-PAGE for reasons that remain unclear.

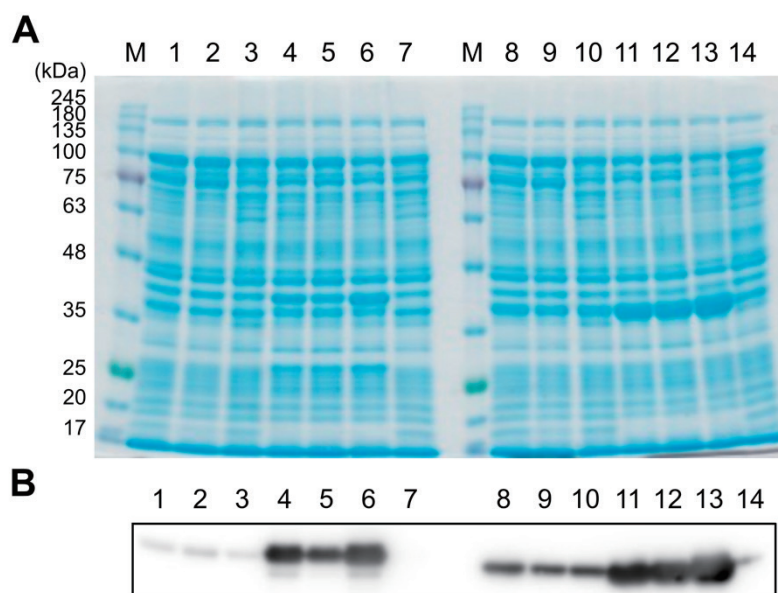


**Figure 5. Optimization of expression conditions for HinSelD and EcoSelD**

Crude cell extracts (8  $\mu$ g of protein each) from *E. coli* BL21(DE3) cells carrying either pHinSelD (lanes 1–6) or pEcoSelD (lanes 8–13) were separated on 10% SDS-PAGE gel, stained with CBB (A), and analyzed by Western blotting using an anti-His tag antibody (B). The cultivation conditions were as follows: 0.4% lactose, 37°C, static (lanes 1 and 8); 0.4% lactose, 30°C, static (lane 2 and 9); 0.4% lactose, 37°C, shaking (lane 3 and 10); 0.1 mM IPTG, 37°C, static (lane 4 and 11); 0.1 mM IPTG, 30°C, static (lane 5 and 12); and 0.1 mM IPTG, 37°C, shaking (lane 6 and 13). Lanes M represent the protein marker, while lanes 7 and 14 correspond to crude extracts of *E. coli* BL21(DE3) cells without plasmid, cultivated with 0.1 mM IPTG at 37°C under shaking conditions.

### Effects of HinSelD SECIS mutations on Sec insertion in HinSelD

Given that the HinSelD SECIS was functional for a read-through of the UGA codon as Sec in the *E. coli* host, we investigated to determine which regions of the HinSelD SECIS are critical for Sec insertion. By comparing the nucleotide sequences of HinSelD SECIS and EcoSelD SECIS, we designed four HinSelD expression plasmids containing different SECIS variants (**Figure 6**). The first mutant, G69A, involved changing the G in the apical loop of HinSelD SECIS to A, as seen in *E. coli*. The second mutant, A75G, involved altering the upper UA base pair in the upper stem to UG. The third mutant, G77A, involved changing the CG base pair in the lower stem to CA, and the fourth mutant, U84C, involved altering the AU base pair in the lower stem to AC. Additionally, we designed a Sec16Cys mutant enzyme by changing the UGA codon for Sec to UGC for Cys. Using the MXfold2 Server [15], we predicted the secondary structures of these SECIS mutants (G69A, A75G, G77A, U84C) (**Figure 6B**).

*E. coli* BL21(DE3) was transformed with expression plasmids containing these HinSelD SECIS variants, and the



expression was induced under the conditions mentioned above. The crude extracts were analyzed by SDS-PAGE and Western blot using anti-His tag antibody, and the results are shown in **Figure 7**. Compared to the wild-type HinSelD, all SECIS variants showed decreased expression levels (69–93%). Notably, the G77A mutant exhibited a significant reduction, with expression levels dropping to approximately 69% of the wild type. This was surprising, given that the four base pair stem immediately below the apical loop was predicted to be retained in G77A (**Figure 6B**), predicting a minimal impact [6]. The G69A mutation had the least impact, with expression levels at 93% of the wild type. This result is consistent with the consensus bacterial SECIS model proposed by Zhang and Gladyshev, which requires at least one G among the first two nucleotides in the apical loop [6]. The A75G mutant, predicted to have the most divergent secondary structure from the wild type (**Figure 6D**) and to disrupt the typically essential four base pairs immediately below the apical loop [6], had an impact of about 81% levels on expression. The U84C mutant, which introduced a mutation in the lower stem [6], was presumed to have a mild effect due to the presence of base pairs above and below the mutation site; however, it showed expression levels at 69% of the wild type. None of the mutations caused a drastic decrease in expression, suggesting that significant effects may require multiple mutations. This also implies a degree of flexibility in recognizing SECIS in Sec-type SelD in *E. coli*. On the other hand, the Sec16Cys mutant exhibited expression levels comparable to the wild-type HinSelD and EcoSelD, indicating that the translation efficiency of UGA for Sec is similar to that of UGC for Cys (**Figure 7**). This result suggests that while the SECIS is maintained in the Sec16Cys mutant, the secondary structure of the SECIS does not inhibit the translation of the preceding UGC codon for Cys.

In conclusion, there is strong conservation between the UGA Sec codon and the SECIS secondary structures in *selD* genes. Although nucleotide differences between the HinSelD and EcoSelD SECIS regions play important roles in UGA translation efficiency, with varying impacts depending on their positions, there is also a degree of flexibility in SECIS recognition in Sec-type SelD in *E. coli*. These findings contribute to a deeper understanding of the mechanisms underlying SECIS recognition and the evolution of SECIS elements in bacteria.

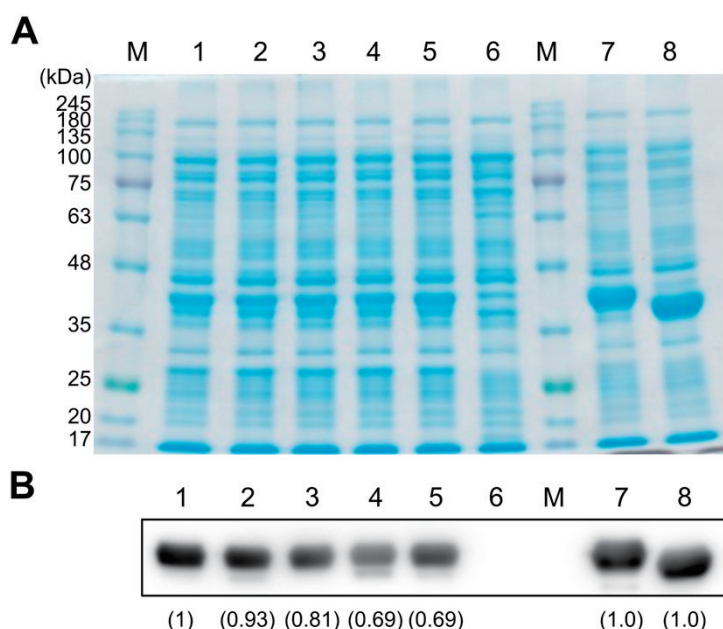


**Figure 7.** Comparison of expression levels of mutant HinSelDs in *E. coli* host cells

Crude cell extracts (8  $\mu$ g of protein each) from *E. coli* BL21(DE3) cells expressing wild-type HinSelD (lane 1), G69A (lane 2), A75G (lane 3), G77A (lane 4), U84C (lane 5), Sec16Cys (lane 7), and EcoSelD (lane 8) were separated on 10% SDS-PAGE gel, stained with CBB (A), and analyzed by Western blotting using an anti-His tag antibody (B). Lanes M contain the protein marker, and lane 6 corresponds to the crude extracts of *E. coli* BL21(DE3) cells without plasmid. The band intensities were quantified using ImageJ software based on Western blot analysis.

## Acknowledgments

This study was supported by KAKENHI grants from the JSPS (JP22K19163 and JP22H04823 to HM), by JST, ACT-X Grant Number JPMJAX22B2, Japan (to MI), and the Ritsumeikan Global Innovation Research Organization, the Program for the Fourth-Phase R-GIRO Research (to HM).

## References

- [1] Stadtman TC. Biosynthesis and function of selenocysteine-containing enzymes. *J Biol Chem*. 1991; 266: 16257-16260.
- [2] Forchhammer K, Böck A. Selenocysteine synthase from *Escherichia coli*. Analysis of the reaction sequence. *J Biol Chem*. 1991; 266: 6324-6328.
- [3] Leinfelder W, Zehelein E, Mandrand-Berthelot MA, Böck A. Gene for a novel tRNA species that accepts L-serine and cotranslationally inserts selenocysteine. *Nature*. 1988; 331: 723-725.
- [4] Ehrenreich A, Forchhammer K, Tormay P, Veprek B, Böck A. Selenoprotein synthesis in *E. coli*. Purification and characterisation of the enzyme catalysing selenium activation. *Eur J Biochem*. 1992; 206: 767-773.
- [5] Baron C, Heider J, Böck A. Interaction of translation factor SELB with the formate dehydrogenase H selenopolypeptide mRNA. *Proc Natl Acad Sci USA*. 1993; 90: 4181-4185.
- [6] Zhang Y, Gladyshev VN. An algorithm for identification of bacterial selenocysteine insertion sequence elements and selenoprotein genes. *Bioinformatics*. 2005; 21: 2580-2589.
- [7] Lacourciere GM, Stadtman TC. Catalytic properties of selenophosphate synthetases: comparison of the selenocysteine-containing enzyme from *Haemophilus influenzae* with the corresponding cysteine-containing enzyme from *Escherichia coli*. *Proc Natl Acad Sci USA*. 1999; 96: 44-48.
- [8] Kim IY, Veres Z, Stadtman TC. *Escherichia coli* mutant SELD enzymes. The cysteine 17 residue is essential for selenophosphate formation from ATP and selenide. *J Biol Chem*. 1992; 267: 19650-19654.
- [9] Altschul SF, Gish W, Miller W, Myers EW, Lipman DJ. Basic local alignment search tool. *J Mol Biol*. 1990; 215: 403-410.
- [10] Kumar S, Stecher G, Tamura K. MEGA7: Molecular evolutionary genetics analysis version 7.0 for bigger datasets. *Mol Biol Evol*. 2016; 33: 1870-1874.
- [11] Minh BQ, Schmidt HA, Chernomor O, Schrempf D, Woodhams MD, von Haeseler A, Lanfear R. Corrigendum to: IQ-TREE 2: New models and efficient methods for phylogenetic inference in the genomic era. *Mol Biol Evol*. 2020; 37: 2461.
- [12] Guindon S, Dufayard JF, Lefort V, Anisimova M, Hordijk W, Gascuel O. New algorithms and methods to estimate maximum-likelihood phylogenies: assessing the performance of PhyML 3.0. *Syst Biol*. 2010; 59: 307-321.
- [13] Minh BQ, Nguyen MA, von Haeseler A. Ultrafast approximation for phylogenetic bootstrap. *Mol Biol Evol*. 2013; 30: 1188-1195.
- [14] Letunic I, Bork P. Interactive Tree of Life (iTOL) v6: recent updates to the phylogenetic tree display and annotation tool. *Nucleic Acids Res*. 2024; 52: W78-W82.
- [15] Sato K, Akiyama M, Sakakibara Y. RNA secondary structure prediction using deep learning with thermodynamic integration. *Nat Commun*. 2021; 12: 941.
- [16] Schneider CA, Rasband WS, Eliceiri KW. NIH Image to ImageJ: 25 years of image analysis. *Nat Methods*. 2012; 9: 671-675.

## Supplementary data

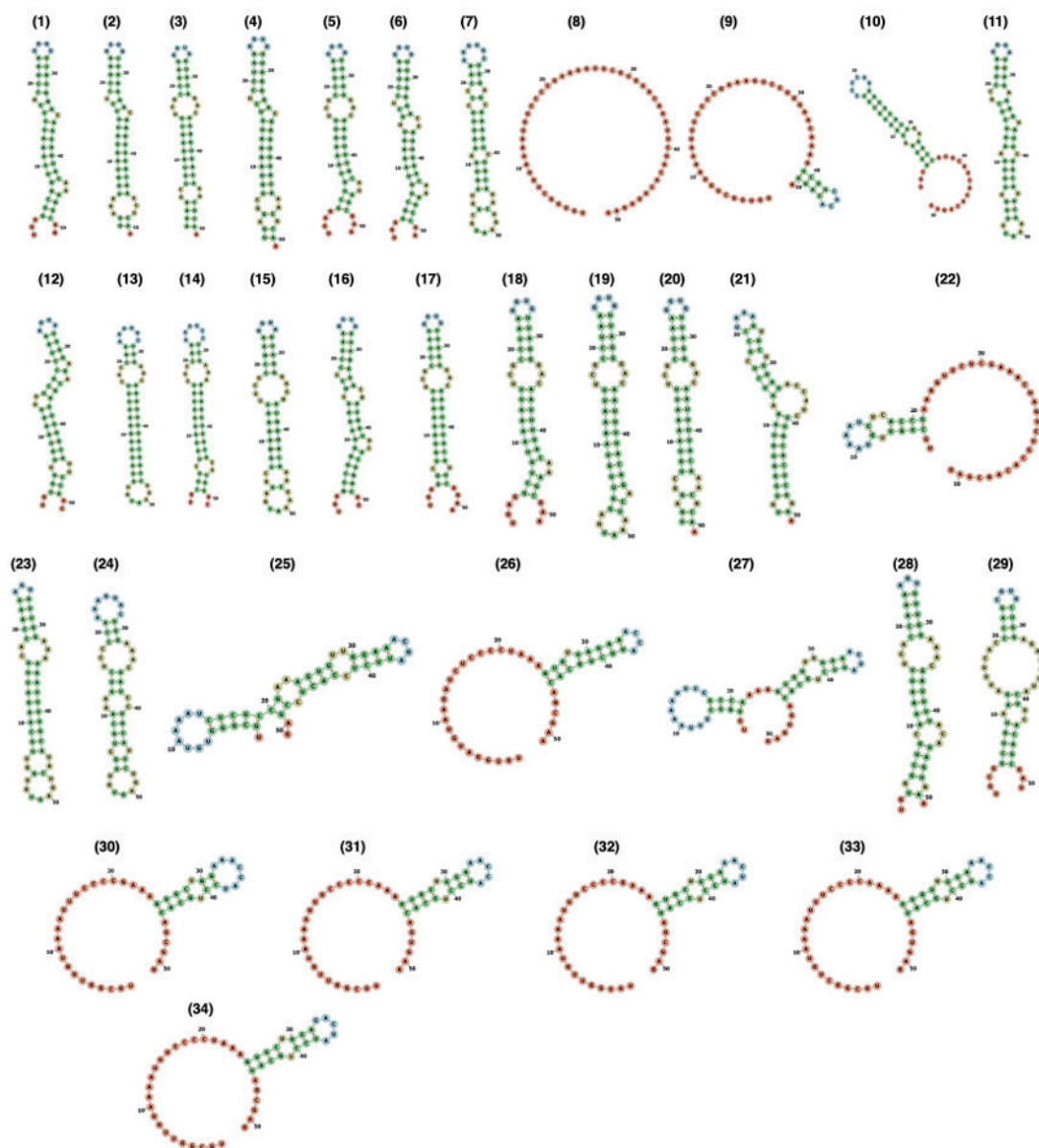


**Figure S1. Prediction of the secondary structure of *selD* SECIS and corresponding regions**

SECIS-like sequences were extracted from 34 *selD* nucleotide sequences, and RNA secondary structure prediction was performed using the MXfold2 Server (<http://www.dna.bio.keio.ac.jp/mxfold2/>). The origin of each SECIS sequence is as follows: *Actinobacillus suis* (1, ASU1\_05425), *Mannheimia bovis* (2, ICJ55\_09770), *Mannheimia haemolytica* (3, D648\_7310), *Mannheimia ovis* (4, GM695\_09155), *Haemophilus parahaemolyticus* (5, E5Q53\_02265), *Actinobacillus porcitosillarum* (6, DDU33\_06660), *Glaesserella* sp. 15-184 (7, CJD39\_01930), *Actinobacillus indolicus* (8, EXH44\_09840), *Glaesserella parasuis* (9, HAPS\_0664), *Gallibacterium anatis* (10, UMN179\_00129), *Aggregatibacter actinomycetemcomitans* (11, ANH9381\_1552), *Pasteurella aerogenes* (12, NCTC13378\_00962), *Pasteurella dagmatis* (13, 4362423\_01086), *Pasteurella multocida* (14, PM0790), *Actinobacillus succinogenes* (15, Asuc\_1749), *Mannheimia succiniciproducens* (16, MS1241), *Haemophilus influenzae* (17, R2866\_0388), *Haemophilus pittmaniae* (18, NCTC13334\_01230), *Haemophilus parainfluenzae* (19, PARA\_00030), *Rodentibacter heylüi* (20, FEE42\_11980), *Plesiomonas shigelloides* (21, SAMEA2665130\_2106), *Serratia proteamaculans* (22, Spro\_2720), *Yersinia pestis* (23, YPO2164), *Jinshanibacter zhutongyuüi* (24, EKN56\_04870), *Leminorella richardii* (25, NCTC12151\_01459), *Hafnia alvei* (26, AT03\_10065), *Xenorhabdus bovienii* (27, XBW1\_2237), *Proteus mirabilis* (28, PMI1497), *Erwinia billingiae* (29, EbC\_24140), *Cronobacter turicensis* (30, CTU\_18100), *Enterobacter cloacae* (31, ECL\_02462), *Klebsiella pneumoniae* (32, KPN\_01207), *Escherichia coli* (33, b1764), *Salmonella enterica* (34, STY1817).